Particle & Particle Systems Characterization
www.particle-journal.com

Controllable and Predictable Viscoelastic Behavior of 3D Boron-Doped Multiwalled Carbon Nanotube Sponges

Wenjie Zhao, Ana L. Elias, Lakshmy P. Rajukumar, Hyung-Ick Kim, Daniel J. O'Brien, Brandon K. Zimmerman, Evgeni S. Penev, Mauricio Terrones, Boris I. Yakobson, Bingqing Wei, X. Lucas Lu, and Jonghwan Suhr**

3D carbon nanotube (CNT)-based macrostructures are the subject of extensive attention because the outstanding properties of 1D and 2D nanostructures have not been fully translated into key engineering applications. Generation of 3D CNT architectures with covalent junctions could endow the new materials with extraordinary mechanical properties. In this study, detailed experimental characterization and statistical comparison are carried out on 3D boron-doped multiwalled CNT (CB_xMWNT) sponges with covalent junctions and undoped multiwalled CNT (undoped-MWNT) sponges without junctions. By investigating the plastic, elastic, viscoelastic, and dynamic viscoelastic properties of both sponges, as well as the dependency of these mechanical properties on material morphology, the CB_xMWNT sponge is found to be a more predictable and stable material than the undoped-MWNT sponge. Statistical comparison proves that the excellent properties of the CB_xMWNT are attributed to its "elbow-like" junctions inside the 3D networks, which prevent permanent buckling and bundling of the CNTs under extreme loading. Thus, by optimizing the covalent junctions in 3D CNT sponges, their functional behavior can be controlled and regulated. These findings may promote applications of 3D CNT sponges in various fields, including biomedical or high-precision devices in which lightweight, controllable, and reliable mechanical properties are always desirable.

Carbon nanotubes (CNTs) and graphene possess outstanding mechanical, electrical, and thermal properties.[1–3] However, translation of the strong mechanical properties, excellent thermal conductivity, and chemical stability of CNTs into real-world applications remains challenging. CNT architectures, ensembles of individual nanotubes, have been widely explored for their potential use in various areas.[4–7] With recent technical advances in nanotube synthesis, such as chemical vapor deposition and solution chemistry techniques, there is a rapidly growing interest in macroscale 3D nanotube architectures.[8–11] In contrast to uniformly aligned nanotube arrays, randomly entangled 3D networks can be considered isotropic and homogeneous materials. A number of research groups have synthesized CNT aerogels.[8,12–14] Covalently bonded 3D hierarchical CNT sponges have been successfully fabricated as well,[9–11] in which CNTs can function as "building blocks" and be "welded" together with molecular junctions.[15–17]

Dr. W. Zhao, B. K. Zimmerman, Prof. B. Wei, Prof. X. L. Lu
Department of Mechanical Engineering
University of Delaware
Newark, DE 19716, USA
E-mail: xlu@udel.edu
Dr. A. L. Elias, Prof. M. Terrones
Department of Physics and Center for
2-Dimensional and Layered Materials
The Pennsylvania State University
104 Davey Lab, University Park, PA 16802-6300, USA
L. P. Rajukumar, Prof. M. Terrones
Department of Materials Science and Engineering
The Pennsylvania State University
104 Davey Lab, University Park, PA 16802-6300, USA
Dr. H.-i. Kim
Region Advanced Manufacturing Technology Agency
Korea Institute of Industrial Technology
Jinju 660-805, Republic of Korea
Dr. D. J. O'Brien
Weapons and Materials Research Directorate
U.S. Army Research Laboratory
Aberdeen Proving Ground, MD 21005, USA
Dr. E. S. Penev, Prof. B. I. Yakobson
Department of Materials Science and NanoEngineering
Rice University
Houston, TX 77005, USA
Prof. M. Terrones
Research Center for Exotic Nanocarbons (JST)
Shinshu University
Wakasato 4-17-1, Nagano 380-8553, Japan
Prof. J. Suhr
Department of Polymer Science and Engineering
Department of Energy Science
Sungkyunkwan University
300 Chunchun-dong, Jangan-gu, Suwon 440-746, South Korea
E-mail: suhr@skku.edu

DOI: 10.1002/ppsc.201500136

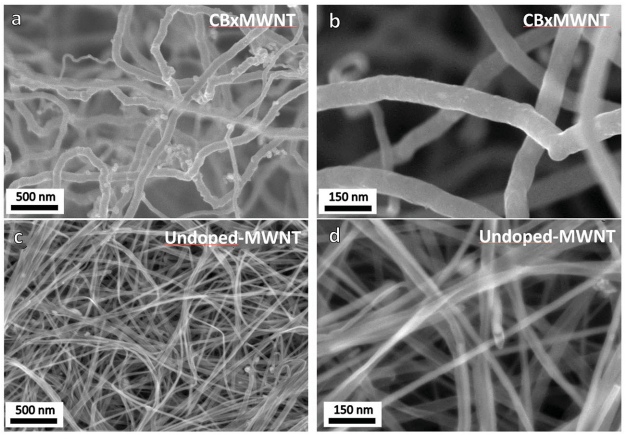

Figure 1. SEM images of the as-grown sponges. a,b) Images showing the morphology of CB_xMWNT sponges and c,d) undoped-MWNT sponges.

Hashim et al. used boron as a dopant in CNTs and successfully created "elbow-like" covalent junctions.[10] Shan et al. synthesized 3D nitrogen-doped CNT sponges by doping both nitrogen and sulfur into CNTs.[11] Given that various 3D CNT structures have been recently fabricated, it is necessary to characterize the macro (or apparent) mechanical properties of 3D CNT architectures and to identify the beneficial effects of transferring the extraordinary properties of nanotubes from 1D to 3D architectures. However, there is currently little knowledge available on the mechanical behaviors of 3D CNT sponges and the impact of CNT covalent interconnections.

In this study, we hypothesize that the covalently bonded junctions could serve as an essential structural element to provide controllable properties as well as structural reliability to the porous 3D CNT sponges. To test this hypothesis, materials of interest include 3D boron-doped multiwalled carbon nanotube sponges (CB_xMWNT) with elbow-like junctions as well as 3D noncovalent multiwalled carbon nanotube sponges (undoped-MWNT), both fabricated with random and entangled nanotube networks. Using a custom-built micro-testing apparatus and a dynamic mechanical analyzer (DMA), the plastic, elastic, viscoelastic, and dynamic viscoelastic properties of both CB_xMWNT and undoped-MWNT sponges were measured. Comparison of the results provides information regarding structure–function relationship for 3D MWNT sponges and offers insight into the roles that covalent junctions play in the mechanical behaviors of the CB_xMWNT sponges.

The structural morphologies of CB_xMWNT and undoped-MWNT sponges fabricated for this study were examined by scanning electron microscopy (SEM). **Figure 1**a,b shows the entangled nature of the CB_xMWNT sponges, with elbow-like junctions clearly visible. CNT covalent junctions in these samples have also been observed, as reported previously.[10] In contrast, CNTs in undoped-MWNT sponges are mostly straight along their length with no covalent or elbow-like junctions (Figure 1c,d). The average diameters of the undoped-MWNTs and CB_xMWNT are measured as ≈20 and ≈70 nm, respectively.

Plasticity represents a material's irreversible deformation under mechanical or thermal loading, and is a key criterion in assessing a material's functional capability, particularly for as-grown MWNT sponges with a high porosity. A

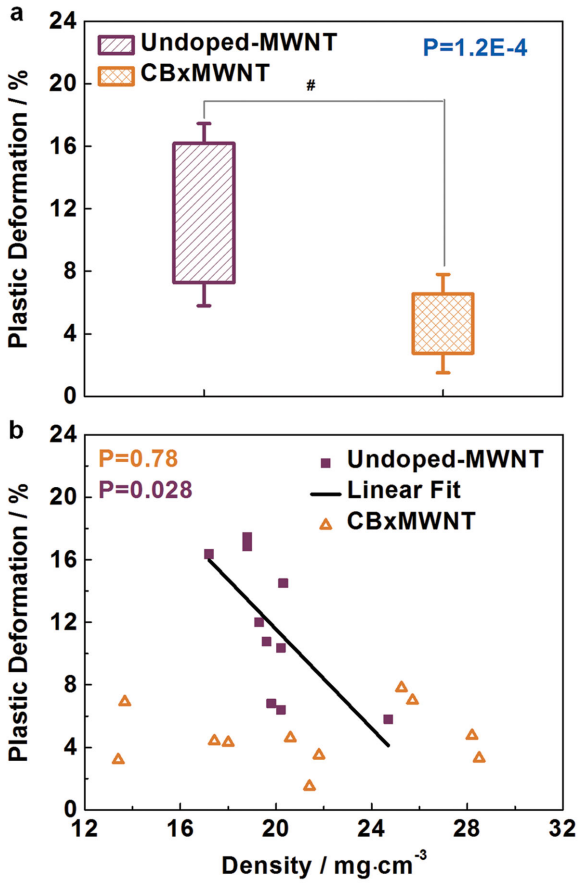

Figure 2. a) Plastic deformation of CB_xMWNT and undoped-MWNT sponges presented in a box-and-whisker plot. # indicates a statistically significant difference between CB_xMWNT and undoped-MWNT sponges ($P < 0.001$). b) The plastic deformation of CB_xMWNT and undoped-MWNT sponges plotted as a function of density. The black line indicates a significant linear correlation between the plastic deformation and apparent density of the undoped-MWNT sponges ($P = 0.028$). Significance is defined as $P < 0.05$.

60% compressive strain was applied to a cylindrical MWNT sponge directly after fabrication, and the new dimensions of the sponge were measured after 24 h recovery. The plastic deformation of the undoped-MWNT sponges was determined as 12 ± 4.4%, while that of the CB_xMWNT sponges was only 5 ± 1.9% (**Figure 2**a). A Student's *t*-test of the data confirmed the significant difference in plastic deformation between the two materials ($P < 0.001$).[18] Considering the highly entangled CNTs in undoped-MWNTs, its large plastic deformation under compression may be attributed to a combination of rearrangement, buckling, and aggregation of CNTs.[19] It has been shown that, under compression, the reestablished van der Waals (vdW) forces can often form bundles of CNTs.[20] However, the covalently bonded junctions in the CB_xMWNT sponges are able to partially overcome the effect of such vdW forces, enable more complete recovery via a purely elastic mechanism, and result in fewer buckled and bundled CNTs inside the structure after an overwhelming compression.[10]

The plastic deformation with respect to the density of sponges is plotted in Figure 2b. Linear regression analysis showed that

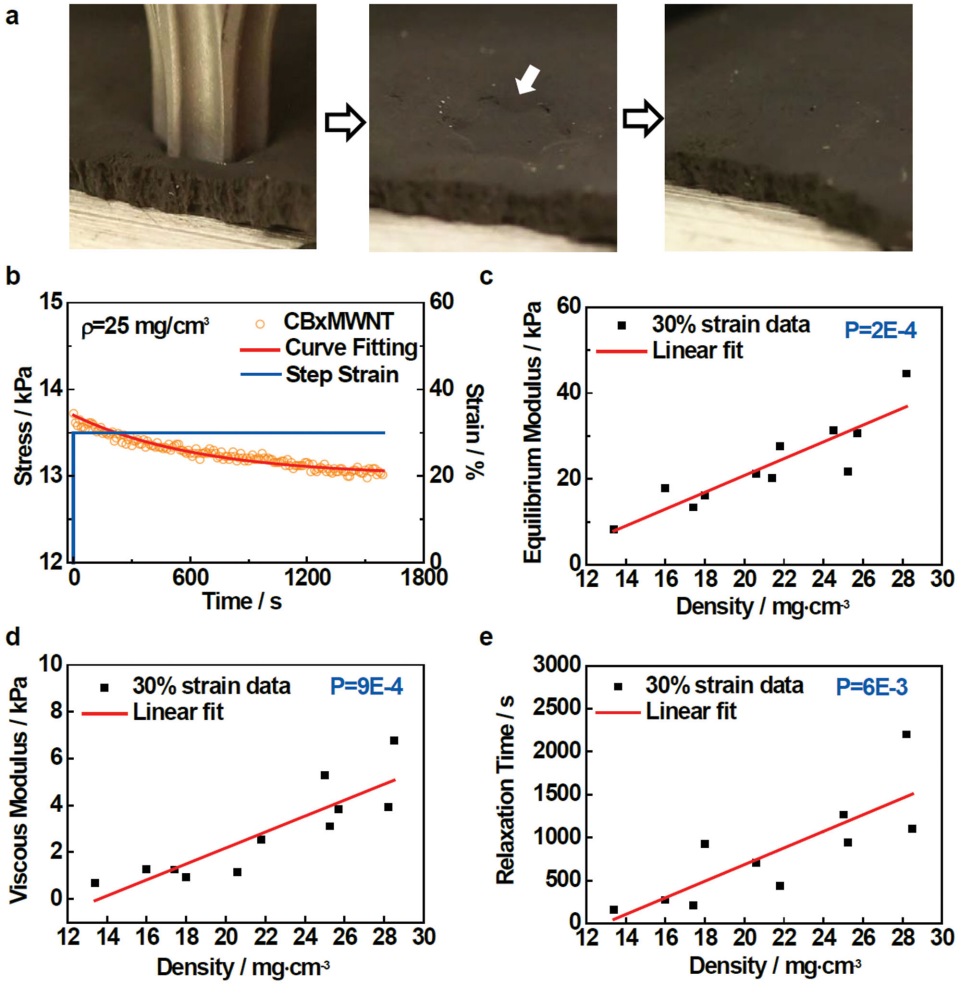

Figure 3. a) Viscoelastic behavior of CB_xMWNT sponge. The sponge was indented within the elastic region, and a noticeable indent (white arrow) was observed immediately after unloading. Deformation almost disappeared a half hour later. b) A representative stress relaxation response curve for a CB_xMWNT sponge under constant compressive strain. The relaxation response was fitted with a standard linear solid model. c–e) Equilibrium modulus, viscous modulus, and relaxation time of CB_xMWNT sponges under 30% compressive strain, plotted as a function of the sponge density.

the undoped-MWNT sponges exhibit a strong negative relationship between the plasticity and density. In contrast, the plastic deformation of CB_xMWNT sponges is density-independent (p = 0.78). As discussed above, the "elbow-like" covalent junctions in the CB_xMWNT sponges could endow the material with much greater resistance to compressive loading, thereby giving rise to density-independent dimensional recoverability. Since the undoped MWNTs do not have covalent junctions and the straight nanotubes are overlapped inside the networks, the sponge with larger porosity (less bulk density) would experience more rearrangement and aggregation under compression, which results in larger plastic deformation. Since the as-fabricated plasticity is not desirable in most applications, the feature of uncoupled density and plasticity makes the behavior of newly fabricated CB_xMWNT sponges more predictable.

The stress–strain relations for both CNT sponges were characterized with quasi-static compressive (1 μm s^{-1}) cyclic loadings. Hysteresis responses in both undoped-MWNT and CB_xMWNT sponges were noted, similar to a number of CNT structures (Figure S1, Supporting Information).[19,22–24] Atomistic molecular dynamics simulations of the CNT systems, mimicking CB_xMWNT sponges (Figure S2, Supporting Information), show a qualitatively similar mechanical response with well-expressed hysteresis. **Figure 3**a demonstrates the typical viscoelastic or "memory foam" behavior of CB_xMWNT sponges. A stress relaxation curve from a CB_xMWNT sponge is shown in Figure 3b. Under a constant compressive strain (30%), the resistant stress gradually decreases over time. When the standard linear solid model was employed to curve-fit the stress relaxation data, the time constant (stress relaxed to 1/e of the peak value) was ≈20 min. The stress relaxation response of the CNT sponges was ascribed to microstructural reorganizations, which minimize internal stresses and allow the sponge to accommodate the applied external load.[24] We believe that, as a typical porous elastic material, sponges under compression also push air out of their networks as they deform. Thus, the mechanical behaviors of CNT sponges could follow the constitutive laws of porous elastic materials. The friction force between the solid matrix (CNT networks) and air induces dissipation of energy and the well-known flow-dependent viscous

characteristics, as noted in solid, cork, and many biological soft tissues.[25] It is important to note that the frictional drag between solid and air phases is not sufficient to significantly increase the temperature of material or change the intrinsic viscosity of CNTs.

The stress-relaxation curves for both CNT sponges were further quantified by employing a standard linear solid model to determine the equilibrium modulus, viscous modulus, and relaxation time. Given that the flow-dependent viscoelastic behaviors of porous materials are mainly affected by the porosity of the solid network,[26] the quantified viscoelastic properties were correlated with the sponge bulk density. Linear regression analysis showed that the equilibrium modulus, viscous modulus, and relaxation time of the CB_xMWNT sponges are all correlated with the density (Figure 3c–e). In addition, similar correlations were confirmed at other compressive strain levels, including 40%, 50%, and 60% strain. Thus, all the quantified viscoelastic properties of the CB_xMWNT sponge increase with the sponge density. This important observation implies that a higher density would lead to: i) greater stiffness of CNT sponges with a larger equilibrium modulus; ii) smaller permeability of the sponge, thus resulting in greater frictional forces between the air and CNTs and thus a higher viscous modulus; and iii) increased time required for the dissipation of air pressure gradients, which corresponds to a longer relaxation time. Importantly, the results indicate that the viscoelastic behavior of the CB_xMWNT sponges can be regulated by controlling their bulk densities. Controllable mechanical properties of 3D CNT sponges are of great practical importance for the design and subsequent applications of systems benefiting from viscoelastic behaviors, e.g., the development of artificial biomaterials, vibrational isolators, and microdevices requiring precise controls.[21]

In sharp contrast to the CB_xMWNT sponges, the viscoelastic parameters of the undoped-MWNT sponges were density-independent at almost all compressive strain levels, with the exception of the equilibrium modulus under high compression (Figure S3, Supporting Information). Therefore, the mechanical properties of the undoped-MWNT sponges appear to be more difficult to control (to any useful degree) with respect to density. Comparison of the results presented here clearly implied that the presence of covalent boron-doped junctions endowed fundamentally new features to 3D CNT networks. The viscoelastic properties for both sponges under different loading conditions are summarized in Figure S4 (Supporting Information). The equilibrium compressive modulus of undoped-MWNT sponges is significantly higher than that of CB_xMWNT sponges, i.e., the presence of elbow-like junctions may reduce the modulus of CNT networks. Although the elbow-like junctions can provide elastic resistance to compression, it may also alter the load supporting mechanisms inside the compressed networks. A thorough understanding of this issue may require further investigation of the junction stiffness and topology of CNTs.

In addition to the static viscoelastic properties, dynamic viscoelastic properties of the two sponge types were characterized using DMA. As before, the dynamic viscoelastic properties of the CB_xMWNT sponges were proved to be density-dependent (40% mean compressive strain, 1% strain amplitude, 1 Hz). The storage modulus and loss factor increase with higher density (**Figure 4**a,b). All measured properties of the undoped-MWNT sponges were still independent of the bulk density (Figure S5, Supporting Information), as there are no covalent junctions along the CNTs. This prominent disparity between the two sponge types was confirmed under multiple mean compressive strain levels (20%, 30%, and 50%), and implies the contribution of covalent junctions to the load–support capability of CNT sponges. It is readily found that the storage modulus, as a measurement of stiffness, increases with density. Meanwhile, CNT sponges with higher densities have increased intertube friction and energy dissipation due to air movement during cyclic compression, resulting in larger loss moduli. The mechanism responsible for a density-dependent loss factor may be explained by the "zipping and unzipping" model proposed previously, which interprets the dissipated energy as the energy consumed to overcome the large vdW attraction between CNTs in unzipping.[27]

Another noticeable feature in Figure 4b is that the loss factor of CB_xMWNT sponges can reach 0.15 at 40% mean compressive strain. Such a high loss factor is comparable to some cellular foams such as polyurethane foam,[28] although the CNT sponge's density is much lower than those of polymer materials. Indeed, the loss factor of the high density CB_xMWNT sponges exceeds 0.1 for all the other mean compressive strains (20%, 30%, and 50%) (Figure S6, Supporting Information). This exciting observation indicates the potential to fabricate an MWNT sponge with a high loss factor merely by controlling the density,[29] which may have various applications; for instance, as a light scaffold for the regeneration of musculoskeletal tissues. At a low mean compressive strain, the loss factor of the undoped-MWNT sponges is comparable to that of the CB_xMWNT sponges (Figure 4c). At >30% mean compressive strain, however, the CB_xMWNT sponge exhibits a significantly higher loss factor than the undoped-MWNT sponge. Therefore, in comparison to undoped-MWNT, the CB_xMWNT sponges may serve as a more superior damping material under dynamic loading.

Figure 4d shows the invariant dynamic viscoelastic properties of both types of sponges in the frequency range of 0.1–10 Hz (strain rate of 4×10^{-3} to 4×10^{-1} s^{-1}). Similar behaviors were observed for CNT sponges undergoing DMA testing in a shear mode.[21,30] Thermal stability of the CNT sponges was confirmed up to 600 °C with thermogravimetric analysis (Figure S7, Supporting Information). The rate-independent and thermally stable viscoelastic behaviors of CNT sponges could broaden their applications in specific engineering and biomedical fields.[31–34]

In this study, the mechanical behavior of 3D undoped-MWNT and CB_xMWNT sponges with atomic-scale junctions was characterized and compared. CB_xMWNT sponges exhibit less (and more stable) plastic deformation than undoped-MWNT sponges, which can be attributed to the outstanding resilience of CB_xMWNT sponges endowed by their covalent junctions. The "elbow-like" junctions prevent the permanent buckling and bundling of CNTs inside the compressed 3D networks by overcoming vdW interactions. Since the quality of crystal lattice of CB_xMWNT is more defective than undoped-MWNT, this could contribute to the distinct mechanical behaviors of two materials observed in this study. Interestingly, the plastic deformation of CB_xMWNT sponges is found to be smaller and

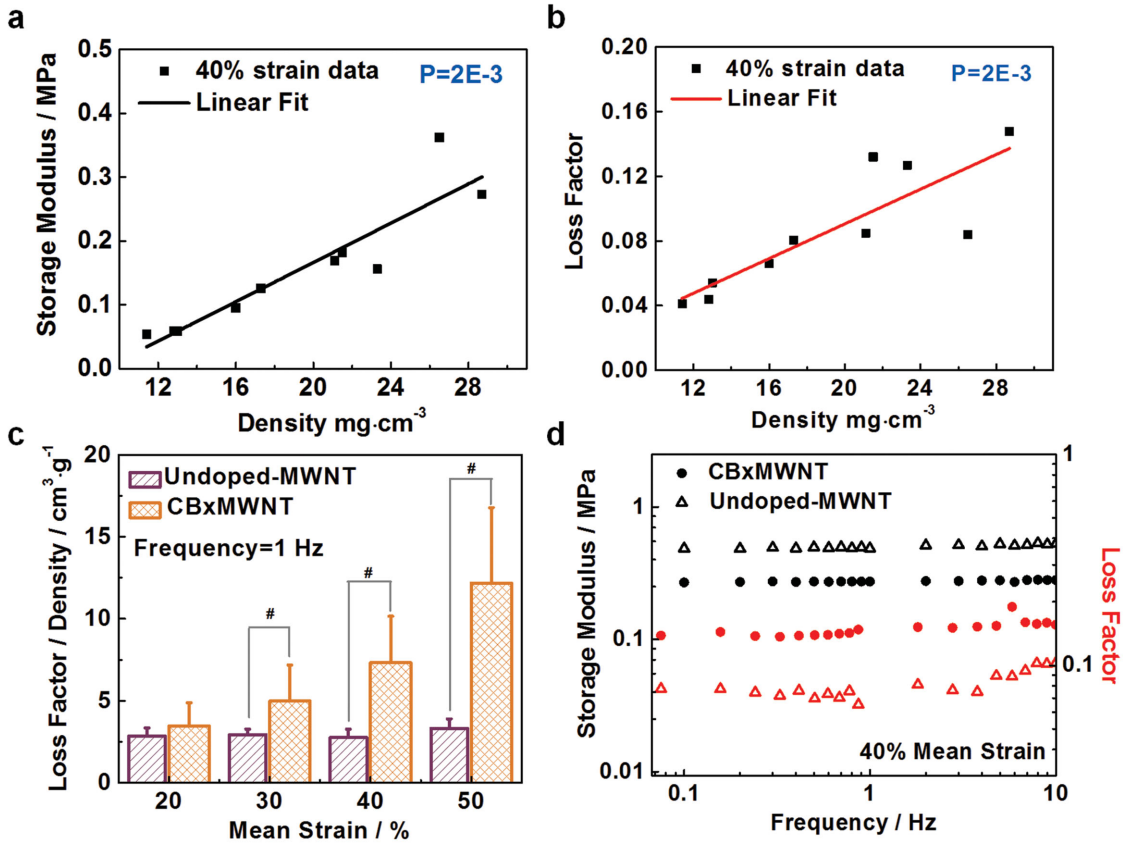

Figure 4. DMA characterization of CB_xMWNT and undoped-MWNT sponges. a,b) Dynamic properties (storage modulus and loss factor) of CB_xMWNT sponges increase with density under dynamic loading at 1 Hz (1% strain over 40% mean compressive strain). c) Density-normalized loss factor of CB_xMWNT and undoped-MWNT sponges (# denotes statistically significant difference). d) Representative dynamic properties (storage modulus and loss factor) of both types of sponges plotted as a function of loading frequency (0.1–10 Hz) at room temperature. Densities of CB_xMWNT and undoped-MWNT sponge sample are 26 and 29 mg cm^{-3}, respectively.

density-independent while that of undoped-MWNT sponges couples with the bulk density. Thus, the failure at defective sites is unlikely the major source of plastic deformation. Moreover, CB_xMWNT sponges exhibit density-dependent properties in both their static and dynamic viscoelastic responses, an effect not seen in the undoped-MWNT sponges. To the best of the authors' knowledge, the controllable viscoelastic properties of 3D CNT structures have not been reported in the literature. A systematic comparison between the mechanical characteristics of undoped-MWNT and CB_xMWNT sponges also revealed a novel direction in controlling the outcome of CNT sponge fabrication, i.e., formation of covalent junctions along CNTs could alter the fundamental structure–function relationship of the material. An abundance of strong evidence proves that the boron-doped junctions endow the CNT sponges with more prominent static and dynamic viscoelastic properties, which could be beneficial in many critical applications, such as biomedical or precision devices, particularly those requiring lightweight, thermally stable materials with controllable viscoelastic behaviors.

Experimental Section

Sample Preparation: Both CB_xMWNT and undoped-MWNT sponges were fabricated according to previous reports.[8,10] CNT samples were cut into cylinders (3 mm diameter) using a Harris Micro-Punch (Ted Pella, Inc.). Thickness of the samples ranged from 0.6 to 1.5 mm. To achieve sufficient statistical power, 11 samples for each type of sponge were tested. An XP6 microbalance (Mettler-Toledo, Inc.) was used to measure the weight of each CNT sample.

As-Fabricated Plastic Deformation: Plastic deformation of each CNT sponge sample was measured using a DMA (Q800, TA Instruments) fitted with 15 mm diameter loading platens. The initial thickness of the sample was determined as the distance between two platens after application of a 0.01 N preload. Next, samples were compressed to 60% strain and held for 1 h, and the thickness was measured again 24 h after the force release. The plastic deformation was calculated as decrease of thickness over initial value.

Viscoelasticity: Stress-relaxation tests were conducted with a custom-built micro-testing apparatus. The cylindrical CNT sample was compressed with a constant step displacement (product of length of CNT samples and the targeted strain), and the load was held for 30 min (Figure 3b). The responsive force history from the sample was recorded. The relaxation tests were performed at 60%, 50%, 40%, and 30% compression in sequence. A 30 min interval time between tests was allowed for the sample to recover to its original length. The recorded stress relaxation curve was fitted with a standard linear solid model,[35] and the equilibrium compressive modulus, viscous modulus, and relaxation time were determined.

DMA Tests: After measuring the initial length of the sponges under the preload, samples were compressed to the desired mean compressive strain (20%, 30%, 40%, or 50%). The sponges were then cyclically compressed and released along their length at constant 1%

strain amplitude. Frequency sweep tests were run at multifrequency mode from 0.1 to 10 Hz.

More detailed description of experiments is addressed in the Supporting Information.

Supporting Information

Supporting Information is available from the Wiley Online Library or from the author.

Acknowledgements

This work was supported by the U.S. Air Force Office of Scientific Research MURI Grant (FA9550–12-1-0035) entitled "Synthesis and Characterization of 3D Carbon Nanotube Solid Networks." J.S. also would like to thank the financial support from the National Research Foundation of Korea (2014R1A2A2A01005496).

Received: July 24, 2015
Revised: September 14, 2015
Published online: November 17, 2015

[1] D. Qian, G. J. Wagner, W. K. Liu, M.-F. Yu, R. S. Ruoff, *Appl. Mech. Rev.* **2002**, *55*, 495.
[2] P. G. Collins, P. Avouris, *Sci. Am.* **2000**, *283*, 62.
[3] Y. Wu, N. Yi, L. Huang, T. Zhang, S. Fang, H. Chang, N. Li, J. Oh, J. A. Lee, M. Kozlov, A. C. Chipara, H. Terrones, P. Xiao, G. Long, Y. Huang, F. Zhang, L. Zhang, X. Lepró, C. Haines, M. D. Lima, N. P. Lopez, L. P. Rajukumar, A. L. Elias, S. Feng, S. J. Kim, N. T. Narayanan, P. M. Ajayan, M. Terrones, A. Aliev, P. Chu, Z. Zhang, R. H. Baughman, Y. Chen, *Nat. Commun.* **2015**, *6*, 6141.
[4] M. Crespo, M. González, A. L. Elías, L. P. Rajukumar, J. Baselga, M. Terrones, J. Pozuelo, *Phys. Status Solidi RRL* **2014**, *8*, 698.
[5] R. K. Das, B. Liu, J. R. Reynolds, A. G. Rinzler, *Nano Lett.* **2009**, *9*, 677.
[6] S. Talapatra, S. Kar, S. K. Pal, R. Vajtai, L. Ci, P. Victor, M. M. Shaijumon, S. Kaur, O. Nalamasu, P. M. Ajayan, *Nat. Nanotechnol.* **2006**, *1*, 112.
[7] B. I. Yakobson, L. S. Couchman, *J. Nanopart. Res.* **2006**, *8*, 105.
[8] X. Gui, J. Wei, K. Wang, A. Cao, H. Zhu, Y. Jia, Q. Shu, D. Wu, *Adv. Mater.* **2010**, *22*, 617.
[9] S. Nardecchia, D. Carriazo, M. L. Ferrer, M. C. Gutierrez, F. del Monte, *Chem. Soc. Rev.* **2013**, *42*, 794.
[10] D. P. Hashim, N. T. Narayanan, J. M. Romo-Herrera, D. A. Cullen, M. G. Hahm, P. Lezzi, J. R. Suttle, D. Kelkhoff, E. Muñoz-Sandoval, S. Ganguli, A. K. Roy, D. J. Smith, R. Vajtai, B. G. Sumpter, V. Meunier, H. Terrones, M. Terrones, P. M. Ajayan, *Sci. Rep.* **2012**, *2*, 363.
[11] C. Shan, W. Zhao, X. L. Lu, D. J. O'Brien, Y. Li, Z. Cao, A. L. Elias, R. Cruz-Silva, M. Terrones, B. Wei, J. Suhr, *Nano Lett.* **2013**, *13*, 5514,
[12] M. A. Worsley, S. O. Kucheyev, J. H. Satcher, A. V Hamza, T. F. Baumann, *Appl. Phys. Lett.* **2009**, *94*, 073115.
[13] X. Gui, A. Cao, J. Wei, H. Li, Y. Jia, Z. Li, L. Fan, K. Wang, H. Zhu, D. Wu, *ACS Nano* **2010**, *4*, 2320.
[14] M. B. Bryning, D. E. Milkie, M. F. Islam, L. A. Hough, J. M. Kikkawa, A. G. Yodh, *Adv. Mater.* **2007**, *19*, 661.
[15] J. M. Romo-Herrera, M. Terrones, H. Terrones, S. Dag, V. Meunier, *Nano Lett.* **2006**, *7*, 570.
[16] J. Li, C. Papadopoulos, J. Xu, *Nature* **1999**, *402*, 253.
[17] M. Terrones, F. Banhart, N. Grobert, J.-C. Charlier, H. Terrones, P. M. Ajayan, *Phys. Rev. Lett.* **2002**, *89*, 75505.
[18] J. H. McDonald, *Handbook of Biological Statistics*, Sparky House Publishing, Baltimore, MD, USA **2009**.
[19] X. Gui, Z. Zeng, A. Cao, Z. Lin, H. Zeng, R. Xiang, T. Wu, Y. Zhu, Z. Tang, *J. Mater. Chem.* **2012**, *22*, 18300.
[20] M. Xu, D. N. Futaba, M. Yumura, K. Hata, *Adv. Mater.* **2011**, *23*, 3686.
[21] M. Xu, D. N. Futaba, T. Yamada, M. Yumura, K. Hata, *Science* **2010**, *330*, 1364.
[22] Q. Zhang, Y. C. Lu, F. Du, L. Dai, J. Baur, D. C. Foster, *J. Phys. D: Appl. Phys.* **2010**, *43*, 315401.
[23] S. D. Mesarovic, C. M. McCarter, D. F. Bahr, H. Radhakrishnan, R. F. Richards, C. D. Richards, D. McClain, J. Jiao, *Scr. Mater.* **2007**, *56*, 157.
[24] J. Suhr, P. Victor, L. Ci, S. Sreekala, X. Zhang, O. Nalamasu, P. M. Ajayan, *Nat. Nanotechnol* **2007**, *2*, 417.
[25] F. Vizesi, C. Jones, N. Lotz, M. Gianoutsos, W. R. Walsh, *J. Hand Surg. Am.* **2008**, *33*, 241.
[26] Y. Kameo, T. Adachi, M. Hojo, *J. Mech. Phys. Solids* **2008**, *56*, 1794.
[27] M. Xu, D. N. Futaba, M. Yumura, K. Hata, *Nano Lett.* **2011**, *11*, 3279.
[28] S. Basu, http://literature.agilent.com/litweb/pdf/5990-9753EN.pdf, (accessed: January 2012).
[29] X. Gui, Z. Lin, Z. Zeng, K. Wang, D. Wu, Z. Tang, *Nanotechnology* **2013**, *24*, 085705.
[30] X. Yang, P. He, H. Gao, *Nano Res.* **2011**, *4*, 1191.
[31] J. Suhr, N. Koratkar, P. Keblinski, P. Ajayan, *Nat. Mater.* **2005**, *4*, 134.
[32] J. Qu, Z. Zhao, X. Wang, J. Qiu, *J. Mater. Chem.* **2011**, *21*, 5967.
[33] M. D. Rao, *J. Sound Vib.* **2003**, *262*, 457.
[34] X. Wei, M.-S. Wang, Y. Bando, D. Golberg, *Sci. Technol. Adv. Mater.* **2011**, *12*, 044605.
[35] W. N. Findley, J. S. Lai, K. Onaran, R. M. Christensen, *Creep and Relaxation of Nonlinear Viscoelastic Materials with an Introduction to Linear Viscoelasticity*, North-Holland Publishing, New York **1976**.